JOURNAL OF PHYSICAL ORGANIC CHEMISTRY
J. Phys. Org. Chem. **12**, 313–318 (1999)

Low-temperature (120 K) structure and vibrational spectrum of protonated proton sponge: the adduct of 1,8-bis(dimethylamino)naphthalene (DMAN) with 4,5-dicyanoimidazole (DCI)

Eugeniusz Grech,[1] Zbigniew Malarski,[2] Wanda Sawka-Dobrowolska[2] and Lucjan Sobczyk[2]*

[1]Institute of Fundamental Chemistry, Technical University, al. Piastów 12, 71-065 Szczecin, Poland
[2]Faculty of Chemistry, University of Wrocław, Joliot-Curie 14, 50-383 Wrocław, Poland

Received 23 March 1998; revised 26 May 1998; accepted 28 May 1998

ABSTRACT: Low-temperature (120 K) studies of the structure of the DMAN·DCI adduct indicate that in symmetrical $[NHN]^+$ hydrogen bridge of 2.571 (1) Å length (2.579(2) Å at room temperature) there is a disorder of the H-atom occupying two positions at nitrogen atoms with a distance of 0.94(3) Å. The comparison with the situation at room temperature seems to show a very low barrier for the proton transfer. The low-frequency vibrations with the participation of the whole $N(CH_3)_2$ groups observed in Raman and inelastic incoherent neutron scattering (IINS) spectra of about 100 cm^{-1} excited at room temperature cause the fundamental level of the protonic mode to penetrate or exceed the barrier. The bending CNC vibrations of about 500 cm^{-1} are strongly coupled with the protonic mode leading to Evans holes in the band ascribed to the $0_+ \rightarrow 0_-$ transition. This hypothesis is consistent with the literature data relating to theoretical studies on $H_3NHNH_3^+$, which show that the barrier for the proton transfer disappears at the hydrogen bond length of about 2.55 Å. Copyright © 1999 John Wiley & Sons, Ltd.

KEYWORDS: protonated proton sponge; low-temperature structure; vibrational spectroscopy

INTRODUCTION

1,8-Bis(dimethylamino)naphthalene (proton sponge; DMAN) and its protonated form in various crystalline setting has evoked continuing interest since the first publication by Alder *et al.*[1] In a review by Bakshi *et al.*[2,] 32 structures containing the DMAN·H^+ cations in the environement of various anions were described. Recently a number of other structures have been reported.[3–11] The N···N hydrogen bond length varies from 2.522(1) to 2.644(2) Å and the NHN angle from 141 to 170°. Symmetrical bridges were found when the cations possess a mirror plane perpendicular to the naphthalene ring in ionic adducts containing $Br^-·H_2O$,[12] tetrazolate·H_2O,[13] $[OTeFe_5]^-$ (140 K),[14] SCN^-,[8] 4,5-dicyanoimidazolate[5] and BF_4^- [15] counter-anions.

In contrast to DMAN itself, the DMAN·H^+ cations are to a large extent flattened with the nitrogen atoms only negligibly displaced from the naphthalene ring plane. An unusually high proton affinity of DMAN and other diamines was theoretically elucidated by Peräkylä.[16]

Of primary importance in the discussion of the DMAN·H^+ cation structure seems to be the shape of the potential for the motion of the bridge proton. The question is whether a single or double minimum exists. X-ray diffraction studies at room temperatures performed so far indicate that the proton occupies one local minimum shifted markedly towards the centre of a bridge. In extreme cases it occupies exactly the central position. Substantial progress in the understanding of the properties of NHN bridges in the DMAN·H^+ cation resulted from low-temperature studies carried out by Kanters and co-workers.[17–19] In three cases, namely DMAN·H^+·nitrate,[17] DMAN·H^+[dihydrogen-hemimellitate]·hemihydrate[18] and $[DMAN·H^+]_2$·[squarate]·tetrahydrate,[18] the difference electron density maps show that at low temperatures there is a double minimum potential. In the first two cases of asymmetric bridges, the population ratios for the two minima are 70:30 and 66:34, respectively, and the N(1)—H and N(2)—H bond lengths corresponding to these minima are close to those usually observed in amino acids.[20] In the case of the squarate salt there is a symmetrical proton distribution between two positions with a distance of about 0.34 Å from the mirror plane. As stated by Sales *et al.*:[17] 'The extremely long N—H distance at room temperature may be interpreted as the result of increased disordering at elevated temperatures.' The disordering of H-atoms in DMAN·H^+ cations

**Correspondence to:* L. Sobczyk, Faculty of Chemistry, University of Wrocław, Joliot-Curie 14, 50-383 Wrocław, Poland.
Contract/grant sponsor: Committee of Scientific Research; *Contract/grant number:* KBN 3T09A 16208.

CCC 0894–3230/99/040313–06 $17.50

was also evidenced by Lopez *et al.*[10] in x-ray diffraction and cross-polarization magic angle spinning NMR studies of the DMAN·HPF_6 and DMAN·picric acid ionic adducts. An extended discussion of this problem, based on collected experimental results and semiempirical calculations, was published by Llamaz-Saiz *et al.*,[21] who speak in favour of a double minimum potential for the proton motion. More advanced *ab initio* calculations by Platts *et al.*[22] unequivocally show that protonation of a free DMAN molecule proceeds preferably at one nitrogen atom. The localization of the bridge proton in protonated DMAN was recently analysed based on NMR spectra.[23]

In this work, we studied the problem of the low-temperature behaviour of $[NHN]^+$ bridges in the adduct of DMAN with 4,5-dicyanoimidazole (DCI).[5] In this crystal there are at least dynamically symmetric DMAN·H^+ cations as reflected both in its geometry and in the symmetry of the potential exerted by the crystalline lattice. This symmetrical system is attractive because we have at our disposal information about spectroscopic behaviour, and in particular about inelastic incoherent neutron scattering and Raman spectra in the region of low frequencies.[24] It seemed that just the low-frequency modes related to the motion of whole $(CH_3)_2N$ groups combined with deformation of the naphthalene skeleton at about 100 cm^{-1} are a key factor ruling the behaviour of the DMAN·H^+ cations.

EXPERIMENTAL

A single crystal of DMAN·DCI used for data collection (approximate dimensions $0.35 \times 0.35 \times 0.35$ mm) was obtained from stoichiometric solution in acetonitrile by slow evaporation of the solvent.

All x-ray intensities were collected using a KUMA KM4 four-circle diffractometer with an Oxford Cryosytem Cryostream Cooler and Mo K_α radiation with a graphite monochromator. Cell parameters were obtained from a least-squares fit of the setting angles of 50 reflections in the range $19 < 2\theta < 27°$. The diffraction data were collected at 120 K with the $\omega - 2\theta$ scan technique up to $2\theta = 70°$. The intensities of three standard reflections monitored after each 100 reflections showed a variation of $\pm 2\%$. A total 4129 of reflections were collected, of which $2382 \geq 2\,\sigma(I)$ were used for structure determination. The intensities of the reflections were corrected for Lorentz and polarization factors but not for absorption.

The crystal structure was solved by direct methods using the program SHELXS-86[25] and refined by full-matrix least-squares methods using SHELXL-93[26] with anisotropic thermal parameters for the non-hydrogen atoms. At intermediate stages of the refinement, the difference maps showed 10 H-atoms; they were included with isotropic thermal parameters. At the end of the refinement the position of the bridging proton was identified from a difference Fourier map calculated with the proton omitted from the final model. A double maximum (*ca* 0.75 e $Å^{-3}$) was found in this position. Therefore, in the final refinement, the bridging proton was treated as statistically disordered with an occupancy factor of 0.5. At convergence, the discrepancy factors $R(F)$, $\omega R(F^2)$ and $S(F^2)$ were 0.0415, 0.1106 and 1.056, respectively. The final difference Fourier map was essentially featureless, with largest peak and hole of 0.48 and -0.18 e $Å^{-3}$. Scattering factors were those incorporated in SHELXL-93.

IR spectra were recorded on a Perkin-Elmer model 180 spectrophotometer for DMAN·DCI suspended in Nujol using CsI plates at 80 and 300 K. The temperature dependence of the IR spectra was measured using a low-temperature vacuum attachment and a control system of our own design.

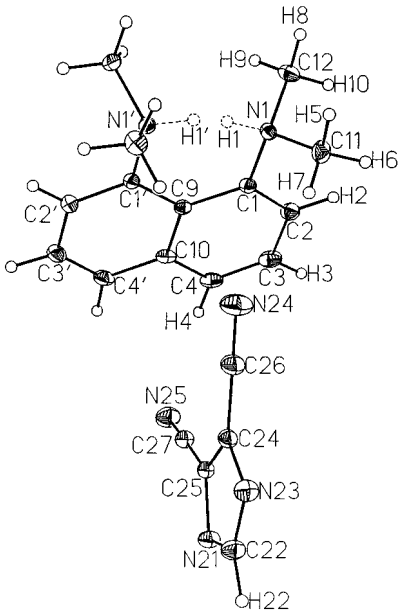

Figure 1. Structure of DMAN·DCI adduct with atom numbering. Symmetry code: (′) *x;* 0.25, *z*

RESULTS AND DISCUSSION

The molecular scheme of the DMAN·DCI adduct with numbering of atoms is shown in Fig. 1 and the packing of molecules in the unit cell is presented in Fig. 2. A summary of crystal data for 293 and 120 K is given in Table 1 and fractional atomic coordinates and equivalent isotropic displacement parameters found at 120 K are collected in Table 2.

Non-hydrogen atomic coordinates with anisotropic displacement parameters, hydrogen atom coordinates with isotropic displacement parameters and bond lengths

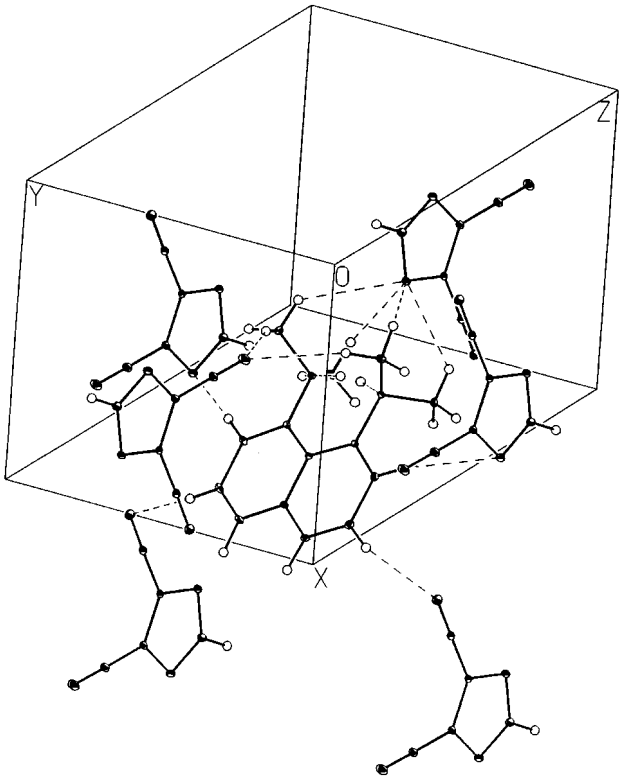

Figure 2. Section of the unit cell showing the molecular packing of DMAN·DCI. Short C—H…N contacts indicated by dashed lines. See Table 4 for geometric data

and angles have been deposited at the Cambridge Crystallographic Data Centre (CCDC No. 101645).

Difference electron density maps within the $[NHN]^+$ bridge calculated for 120 and 293 K are shown in Fig. 3, and a comparison of the geometry of the $[NHN]^+$ hydrogen bridge at 293 and 120 K is presented in Table 3.

Table 1. Summary of crystal data for the 1:1 DMAN.DCI adduct at 293 and 120 K

	293 K	120 K
Crystal system	monoclinic	
Space group	P21/m	
Cell constants		
a (Å)	7.999(3)	7.903(2)
b (Å)	11.566(2)	11.455(2)
c (Å)	10.706(4)	10.587(2)
β (°)	110.51(3)	110.14(2)
V (Å^3)	927.8(5)	899.8(3)
Z	2	2
D_c (g cm^{-3})	1.119(1)	1.227(1)
μ (mm^{-1})	0.59	0.077

The analysis of the material gathered in this work enables us to formulate the following conclusions with respect to the influence of cooling on the structure of DMAN·DCI adduct. First, the temperature does not affect either the lattice symmetry or the symmetry of the DMAN·H$^+$ cation. The $[NHN]^+$ hydrogen bond length shortens on cooling to 120 K by about 0.01 Å and the bridge becomes less bent. The length at 120 K of 2.571(1) Å belongs to very short (but not shortest) $[NHN]^+$ bridges. The temperature does not affect the mutual orientation of planar cations and anions. They are oriented perpendicular to each other, and the symmetry plane of the DMAN·H$^+$ cation includes the planar anion. With respect to the packing density, lowering of the temperature leads to remarkable shortening of contacts between the N-atoms of the cyano groups and C—H bonds of the methyl groups or of the naphthalene skeleton, associated with participation of the imidazole ring nitrogen atoms. Representative data are given in Table 4.

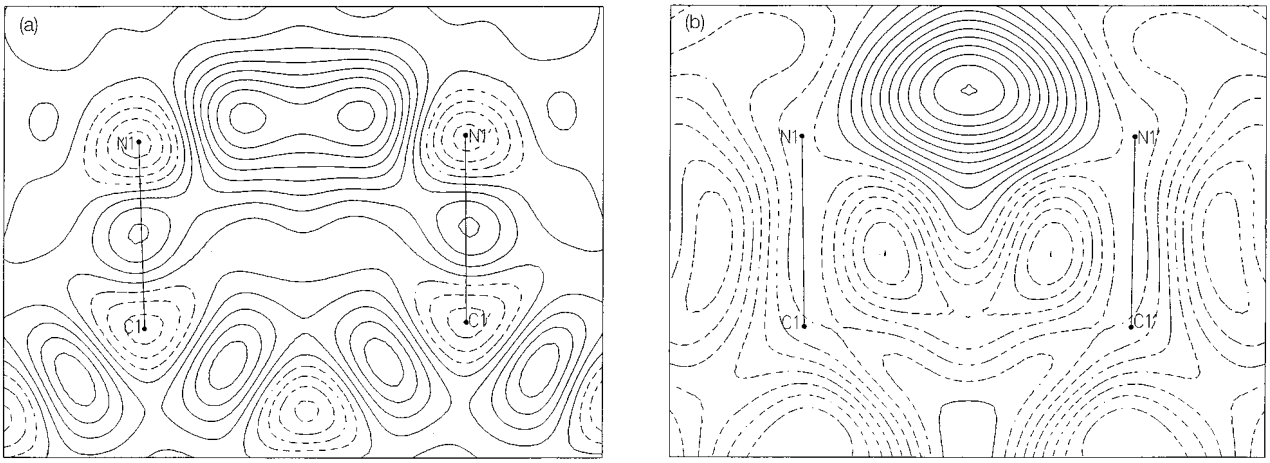

Figure 3. Difference electron density maps within the $[NHN]^+$ bridge calculated with proton omitted from the final model. The molecular fragments marked on the maps were used to define sections for contouring the maps: (a) (120 K) the contour is drawn with 0.1 e Å^{-3} intervals; (b) (293 K) the same with 0.03 e Å^{-3} intervals. Zero and negative lines dashed

Table 2. Fractional atomic coordinates and equivalent isotropic displacement parameters for DMAN.DCI adduct at 102 K

Atom	*x*	*y*	*z*	U_{eq}/U_{iso}
N(1)	0.68436(11)	0.13779(7)	0.36272(8)	0.0174(2)
N(21)	0.4469(2)	0.2500	−0.4469(1)	0.0230(2)
N(23)	0.2090(2)	0.2500	−0.3712(1)	0.0262(3)
N(24)	0.3762(2)	0.2500	−0.0181(2)	0.0436(4)
N(25)	0.8510(2)	0.2500(2)	−0.1760(1)	0.0322(3)
C(1)	0.8013(1)	0.1397(1)	0.2816(1)	0.0170(2)
C(2)	0.8612(2)	0.0375(1)	0.2447(1)	0.0233(2)
C(3)	0.9758(2)	0.0390(1)	0.1677(1)	0.0274(2)
C(4)	1.0270(1)	0.1426(1)	0.1293(1)	0.0248(2)
C(9)	0.8526(2)	0.2500	0.2443(1)	0.0162(2)
C(10)	0.9685(2)	0.2500	0.1663(1)	0.0200(2)
C(11)	0.5072(2)	0.0839(1)	0.2908(1)	0.0261(2)
C(12)	0.7740(2)	0.0839(1)	0.4964(1)	0.0248(2)
C(22)	0.2674(2)	0.2500	−0.4757(2)	0.0262(3)
C(24)	0.3653(2)	0.2500	−0.2637(1)	0.0208(2)
C(25)	0.5104(2)	0.2500	−0.3098(1)	0.0184(2)
C(26)	0.3703(2)	0.2500	−0.1281(2)	0.0284(3)
C(27)	0.6985(2)	0.2500	−0.2344(1)	0.0222(3)
H(1)	0.6716(37)	0.2176(25)	0.3765(29)	0.034(2)

$$U_{eq} = \frac{1}{3}\sum_i \sum_j U_{ij} a_i^* a_j^* a_i a_j$$

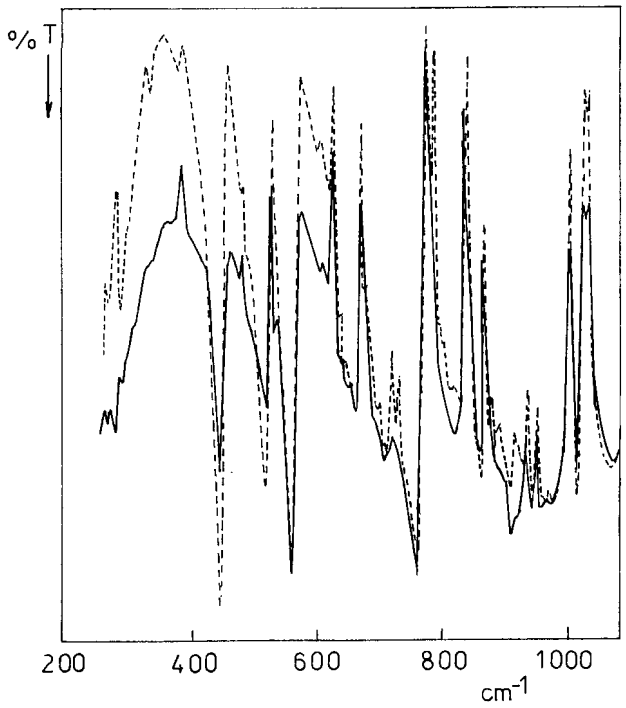

Figure 4. IR absorption spectra of DMAN·DCI in Nujol at 293 K (solidline) and 120 K (dotted line) in the region below 1000 cm^{-1}. The Evans holes are located at 440, 517 and 560 cm

The most salient effect connected with cooling of DMAN·DCI relates to the behaviour of the bridge proton expressed in electron density maps at 293 and 120 K. At 120 K two equivalent positions of the proton are found at a distance of 0.94(3) Å from the nitrogen atoms. This result is similar to that obtained by Kanters *et al.*[19] for another salt of DMAN with a dynamically symmetrical $[NHN]^+$ hydrogen bond with N···N distances of 2.574(3) and 2.594(3) Å at 100 K.

The shape of the potential for the proton motion in $H_3NHNH_3^+$ cations has been analysed theoretically.[27–30] According to the calculations by Scheiner,[29] using the 4–31G basis set within the Hartree–Fock formalism, one could expect the barrier to vanish at an N···N distance of about 2.55 Å. Very similar conclusions can be drawn from the results by Merlet *et al.*[28] and Delpuech *et al.*[27] Although these results cannot be directly transferred to the present work, it seems that in the $DMAN{\cdot}H^+$ cation there is a low barrier hydrogen bonding, and this barrier may be close to *kT*. Hence at low temperatures the zero point vibrational level is located below the barrier and two peaks of the wavefunction should exist, whereas at elevated temperatures this level can exceed the barrier top.

The energetic levels for such bridges were analysed by Merlet *et al.*[28] From the analysis it follows that the four lowest levels, denoted 0, 1, 2 and 3 (corresponding to notation 0_+, 0_-, 1_+ and 1_-) depend strongly on the bridge length and barrier. In the case of a very low barrier the $0_+ \rightarrow 0_-$ transition is a few hundred cm^{-1} and the isotopic ratio can reach anomalously high values. Bridges within this range of length should be most sensitive to the external conditions. The transition moments for $[NHN]^+$ bridges were not analysed but there are data available for $[OHO]^+$ bridges of corresponding geometry. Scheiner[29] showed that $[NHN]^+$ bridges behave similarly to $[OHO]^+$, which are about 0.1 Å shorter. Janoschek *et al.*[31] showed that of two possible transitions, $0_+ \rightarrow 0_-$, and $0_+ \rightarrow 1_-$, the latter is characterized by a probability that is the lower the higher is the barrier. If the distance between

Table 3. Comparison of the geometrical parameters of the $[NHN]^+$ hydrogen bridge in the DMAN.DCI adduct at 293 and 120 K

T(K)	$d(N_1 \ldots N_1^{i})$ (Å)	$d(N_1—H_1)$ (Å)	$d(H_1 \ldots N_1^{i})$ (Å)	$<N_1H_1N_1^{i}$ (°)
293	2.579(2)	1.321(8)	1.321(8)	155(3)
120	2.571(1)	0.94(3)	1.67(3)	160(3)

symmetry code (^{i}): *x*, 0.25, *z*

Table 4. Short C—H···N contacts in DMAN.DCI

C—H···N	d(C···N) (Å)		d(H···N) (Å)		<(C—H···N)(°)	
	293 K	120 K	293 K	120 K	293 K	120 K
C(11)—H(7) ··· N(24)	3.673(3)	3.614(2)	2.73(2)	2.66(2)	167(2)	163(1)
C(11)—H(5) ··· N(21)^{i}	3.596(3)	3.531(2)	2.80(2)	2.82(2)	135(2)	133(1)
C(12)—H(8) ··· N(21)^{i}	3.481(3)	3.425(2)	2.70(2)	2.68(2)	136(2)	139(1)
C(2)—H(2) ··· N(23)^{ii}	3.737(2)	3.669(1)	2.78(2)	2.71(2)	167(2)	169(1)
C(3)—H(3) ··· N(25)^{iii}	3.682(3)	3.571(1)	2.77(2)	2.63(2)	157(2)	161(1)

symmetry code (^{i}) $x,y,z+1$; (^{ii}) l-x,-y,-$z+1$; (^{iii}) 2-x,-y,-z.

the 0_+ and 0_- levels is considerable, then we do not observe transitions from the 0_- levels. Hence in IR spectra without an external electrical field we should observe only one band $0_+ \rightarrow 0_-$ in the range 300–650 cm^{-1}. The low-frequency intense band observed in various protonated sponges is located in this region.[32] Figure 4 shows this section of the IR spectrum at 293 and 120 K for the DMAN·DCI adduct. We do not observe any other absorption above 1000 cm^{-1} which could be ascribed to vibrations of the bridge proton.

The behaviour of the band ascribed to the $0_+ \rightarrow 0_-$ transition in DMAN·H$^+$ can be understood by analysing the low-frequency vibrations related to the motion of the $(CH_3)_2N$ groups. Raman and particularly the IINS studies of the DMAN·DCI adduct show frequencies in the range 30–150 cm^{-1}, which, based on theoretical analysis, should be ascribed to the $(CH_3)_2N$ vibrations with participation of deformations of the naphthalene ring. One can distinguish frequencies of 34, 102, 120 and 156 cm^{-1}. The coupling of the protonic mode with such vibrations should lead, according to Marechal and co-workers[33,34] and Shchepkin,[35] to broadening and in some cases to fine structure of the bands. In our case, owing to additional coupling with lattice vibrations and to the Zundel polarizability, we do not observe such a structure. On the other hand, the Evans holes arising from the coupling with bending NC_3 modes are seen very well. These modes are also observed in IINS spectra in the range 300–700 cm^{-1}. In the IR absorption spectrum of the DMAN·DCI adduct (similar in other DMAN salts), these windows are located at 440, 517 and 560 cm^{-1}.

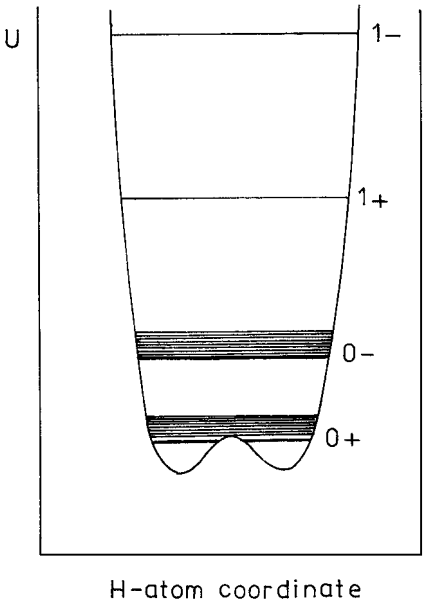

Figure 5. Postulated vibrational protonic levels for the DMAN·H$^+$ cation in the one-dimensional approximation

The coupling of protonic vibrations with low-frequency modes of the $(CH_3)_2N$ groups causes the appearance of additional sub-levels corresponding to these frequencies and their overtones (kT is of the order of 200 cm^{-1} at room temperature). This is presented in the energy diagram in Fig. 5. At room temperature there are possible states exceeding the barrier, as shown by electron density maps and the behaviour of the $0_+ \rightarrow 0_-$ band, which confirm such a hypothesis. A reduction in temperature causes an intensification of that band, particularly in the low-frequency wing. As follows from calculation,[31] the transition moment for the $0_+ \rightarrow 0_-$ transition is the larger the higher is the barrier. Thus the increase in population of low-lying local levels should lead to an enhancement of the integrated intensity, especially in the low-frequency wing.

The working hypothesis that the energetic barrier for the proton transfer in the DMAN·H$^+$ cation is of the order of kT also explains why a very large (much more than $\sqrt{2}$) isotopic frequency ratio is observed in various salts of DMAN.[36] Such an anomalous behaviour is consistent with the calculations by Merlet *et al.*[28] for the $0_+ \rightarrow 0_-$ transition in the $H_3NHNH_3^+$ cation. A high value of the frequency isotopic ratio can also be expected in the case of a double minimum potential with a low barrier based on semiempirical studies using polynomial functions.[37,38] The appearance of broad ('continuous') absorption for DMAN salts in strongly polar solvents such as acetonitrile[32] is due to electrostatic interactions between the cation and dipoles of the solvent molecules. This leads to an asymmetric transient deepening of the minima and an increase in the transition moments to higher protonic levels and their diffusion. In addition,

broadening of bands due to the Zundel polarizability mechanism[39] takes place.

Acknowledgements

Financial support from the Committee for Scientific Research (Grant KBN 3T09A 16208) is acknowledged.

REFERENCES

1. R. W. Alder, A. G. Orpan and R. B. Sessions, *J. Chem. Soc., Chem. Commun.* 999 (1983); R. W. Alder, *Chem. Rev.* **89**, 1215 (1989).
2. P. K. Bakshi, T. S. Cameron and O. Knop, *Can. J. Chem.* **74**, 201 (1996).
3. T. Glowiak, E. Grech, Z. Malarski, J. Nowicka-Scheibe and L. Sobczyk, *J. Mol. Struct.* **381**, 169 (1996).
4. T. Glowiak, E. Grech, Z. Malarski and L. Sobczyk, *J. Mol. Struct.* **403**, 73 (1997).
5. E. Grech, Z. Malarski, W. Sawka-Dobrowolska and L. Sobczyk, *J. Mol. Struct.* **406**, 107 (1997).
6. E. Grech, Z. Malarski, W. Sawka-Dobrowolska and L. Sobczyk, *J. Mol. Struct.* **416**, 227 (1997).
7. E. Grech, Z. Malarski, P. Milart, W. Sawka-Dobrowolska and L. Sobczyk, *J. Mol. Struct.* **436–437**, 81 (1997).
8. E. Bartoszak, M. Jaskólski., E. Grech, T. Gustafsson and I. Olovsson, *Acta Crystallogr., Sect. B* **50**, 358 (1994).
9. K. Woźniak, Ch. C. Wilson, K. S. Knight, W. Jones and E. Grech, *Acta Crystallogr., Sect. B* **52**, 691 (1996).
10. C. Lopez, R. M. Claramunt, A. L. Llamas-Saiz, C. Foces-Foces, J. Elguero, I. Sobrados, F. Aguilar-Parrilla and H. H. Limbach, *New J. Chem.*, **20**, 523 (1996).
11. K. Woźniak, T. M. Krygowski, D. Pawlak, W. Kolodziejski and E. Grech, *J. Phys. Org. Chem.* **10**, 814 (1997).
12. D. Pyżalska, R. Pyżalski, T. Borowiak, *J. Crystallogr. Spectrosc. Res.* **13**, 211 (1983).
13. T. Glowiak, Z. Malarski, L. Sobczyk and E. Grech, *J. Mol. Struct.* **270**, 441 (1992).
14. P. J. Kellet, O. P. Anderson, S. H. Strauss and K. D. Abney, *Can. J. Chem.* **67**, 2023 (1989).
15. K. Woźniak, T. M. Krygowski, B. Kariuki, R. W. Jones and E. Grech, *J. Mol. Struct.* **240**, 111 (1990).
16. M. Peräkylä, *J. Org. Chem.* **61**, 7420 (1996).
17. O. Salas, J. A. Kanters and E. Grech, *J. Mol. Struct.* **271**, 197 (1992).
18. M. L. Raves, J. A. Kanters and E. Grech, *J. Mol. Struct.* **271**, 109 (1992).
19. J. Kanters, A. Schouten, J. Kroon and E. Grech, *Acta Crystallogr., Sect. C* **48**, 1254 (1992).
20. T. F. Koetzle and M. S. Lehmann, in The Hydrogen Bond—Recent Developments in Theory and Experiment, edited by P. Schuster, G. Zundel and C. Sandorfy, Vol. **2**, p. 457. North-Holland, Amsterdam (1976).
21. A. L. Llamas-Saiz, C. Foces-Foces and J. Elguero, *J. Mol. Struct.* **328**, 297 (1994).
22. J. A. Platts, S. T. Howard and K. Woźniak, *J. Org. Chem.* **59**, 4647 (1994).
23. A. F. Pozharskii and V. A. Ozeryanskii, *Izv. Akad. Nauk., Ser. Khim.* 68 (1998).
24. A. Pawlukojć, I. Natkaniec, E. Grech, J. Baran, Z. Malarski and L. Sobczyk, *Spectrochim. Acta, Part A* **54**, 439 (1998).
25. G. M. Sheldrick, *Acta Crystallogr., Sect. A* **46**, 467 (1990).
26. G. M. Sheldrick, SHELXL-93: Program for the Refinement of Crystal Structures. University of Gottingen, Gottingen (1993).
27. J. J. Delpuech, G. Serratrice, A. Strich and A. Veillard, *J. Chem. Soc., Chem. Commun.* 817 (1972).
28. P. Merlet, S. D. Peyerimhoff and R. J. Buenker, *J. Am. Chem. Soc.* **94**, 8301 (1972).
29. S. Scheiner, *J. Phys. Chem.* **86**, 376 (1982).
30. L. Jaroszewski, B. Lesyng, J. J. Tanner and J. A. McCammon, *Chem. Phys. Lett.* **175**, 282 (1990).
31. R. Janoschek, E. G. Weidemann, H. Pfeiffer and G. Zundel, *J. Am. Chem. Soc.* **94**, 2387 (1972).
32. E. Grech, Z. Malarski and L. Sobczyk, *J. Mol. Struct.* **129**, 35 (1985).
33. Y. Marechal and A. Witkowski, *J. Chem. Phys.* **48**, 3697 (1968).
34. G. L. Hofacker, Y. Marechal and M. A. Ratner, in The Hydrogen Bond—Recent Developments in Theory and Experiment, edited by P. Schuster, G. Zundel and C. Sandorfy, Vol. **1**, Chapt. 6, p. **297**. North-Holland, Amsterdam (1976).
35. D. N. Shchepkin, *J. Mol. Struct.* **156**, 303 (1987).
36. E. Grech, Z. Malarski and L. Sobczyk, *Chem. Phys. Lett.* **128**, 259 (1986).
37. H. Romanowski and L. Sobczyk, *Chem. Phys.* **19**, 361 (1977).
38. Y. Guissani and H. Ratajczak, *Chem. Phys.* **62**, 319 (1981).
39. G. Zundel, in The Hydrogen Bond—Recent Developments in Theory and Experiment, edited by P. Schuster, G. Zundel and C. Sandorfy, Vol. **2**, p. **683**. North-Holland, Amsterdam (1976).

